

A Cascaded Tracking Control Concept for Pneumatic Muscle Actuators

A. Hildebrandt*, O. Sawodny*, R. Neumann**, A. Hartmann**

*Institute of Automation and Systems Engineering
Technische Universität Ilmenau
D-98684 Ilmenau, Germany

**Festo AG & Co.
Research Mechatronics
D-73734 Esslingen, Germany

Keywords: Tracking control, nonlinear control, position control, force control, modelling of pneumatic systems.

Abstract

Pneumatic muscles are interesting in their use as actuators in robotics, because they have a high power/weight ratio, a high tension force and a long durability. However, their physical model is highly nonlinear. In this paper a nonlinear control strategy is presented. The main objective is to control a trolley, which is driven by an artificial muscle to follow a reference path. The cascaded control, which is presented here is based on a physical model of an experimental setup. The inner loop is responsible for the force control, which cancels the nonlinearities of the system and ensures therefore a linear input/output behavior. The outer control loop consists of a feedforward and an observer based feedback controller. In addition the observer is extended with a disturbance observer in order to compensate model errors. Measurement results show the efficiency of the presented control strategy.

1 Introduction

Pneumatic actuators are interesting for their use in automation concepts. Unfortunately, due to their excessive nonlinearities [Tak99], a high precision control, especially the trajectory tracking control can not be handled by linear control design methods in a satisfactory way [Neu00]. Advanced control strategies like feedback linearization [Saw02], adaptive control [Tan99] based on neural networks [Tao96] have been investigated and explored. As an alternative to a single action pneumatic cylinder one can use so called pneumatic muscles as actuator for trajectory tracking problems. Compared to cylinders, their main advantages are: high power/weight ratio, usability in rough environments, maintenance free, frictionless, path of action up to 2.5m. A major drawback of fluidic muscles is that they have a position-pressure dependency of the force and a nonlinear position dependency of the volume. These nonlinearities make it difficult to perform accurate position tracking tasks. [Rep99] presented a tracking controller based on gain scheduling. In this approach the muscle is modelled as a two passive element model consisting of a spring element and a viscous element. Nevertheless, the parameters have to be mea-

sured intensively. Furthermore, there are no experimental results shown to evaluate the efficiency of the controller. [Lin99] described the development of an angle controlled mechanical oscillator using a dead-beat proportional discrete controller. The muscle force is hereby modelled in a physical way and depends on many parameters, which are only valid for McKibben [Cho96] muscle. Experimental results show that the controller works relatively slow. [Hil02] presented a physical model of an experimental setup, whereby the parameters are identified experimentally. Using a feedback linearization technique in this approach a position accuracy of 100 μ m is ensured. This paper continues the work on control of fluidic muscles, which is presented in [Hil02]. The motivation is to develop a more accurate and more robust control strategy.

2 System Illustration

In the following, a commercial pneumatic muscle is considered, which was presented in 1999 by the pneumatic manufacturer Festo [Neu01]. It consists of a cylindrical, an isotropic flexible rubber tube and two connection flanges. When the muscle is inflated with compressed air, it widens. Hence a tension force, as well as a contraction movement in the longitudinal direction is created. The muscle is simply a flexible pulling actuator and cannot transmit pressure forces. The tension force is at its maximum at the beginning of the contraction and drops with the stroke to zero. It produces a maximum pulling force at 6bar of 4000N, contracts up to 25% of its rated length and possesses a very long life period of at least 10 million switching cycles. In order to investigate trajectory tracking strategies, an experimental setup using a pneumatic muscle with a rated length of 1.2m and a rated diameter of 40mm was realized. Figure 1 shows the working principles of the test stand. A fluidic muscle drives a trolley, which can be loaded with sand bag in the longitudinal direction. In this configuration the muscle contracts at a relative pressure of $p_{rel} = 6bar$ to $z = 300mm$. Figure 2 shows the essential components of the test stand. In order to influence the pressure and flow rate, an electronic proportional directional control valve in 5/3-way function is used. The in z -direction moving trolley is guided nearly frictionless. An optical position incremental encoder measures the position of the trolley. A pressure sensor gauges the pressure inside the tube.

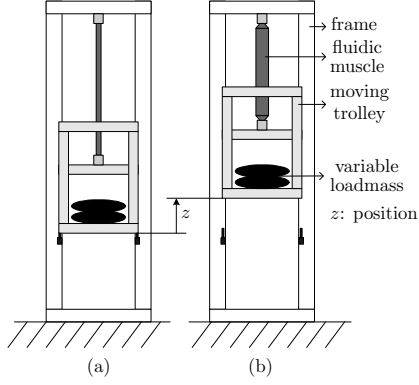


Fig. 1: Explanation of the test stand action; (a) fully deflated muscle (b) inflated muscle.

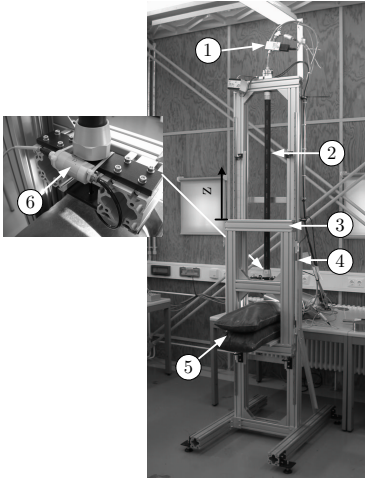


Fig. 2: Experimental setup; z : position of the slide, 1: valve, 2: fluidic muscle (rated length: $1.2m$), 3: moving trolley, 4: position encoder, 5: bags to vary the mass, 6: pressure sensor.

3 System Model

To depict the dynamic and static behavior of the system, a mathematical set of nonlinear equations is derived. The initial point is to describe the pressure inside the muscle in relation to the valves air flow rate. The ideal gas equation describes the dependency of the gas mass:

$$m_g = \frac{pV}{RT}, \quad (1)$$

where m_g =gas mass inside the muscle, p =pressure inside the muscle, V =muscles inner volume, R =specific gas constant, T =gas temperature. Because the muscle tube consists of an elastomer, it can only pass partly the heat through the material. Any variation of the muscle's volume or pressure behave between the ideal condition isothermal and adiabatic and can be described by the polytrophic gas law:

$$p_b V_b^\chi = p_e V_e^\chi = \text{constant}, \quad (2)$$

where the index "b" indicates the beginning and index "e" points the end of the variation of the muscle's volume or pressure. The polytrophic exponent χ is identified to $\chi = 1.26$. The total differential of equation (1) combined with equation (2) form the differential derivative for the pressure:

$$\dot{p} = \frac{\chi}{V} \left(RT\dot{m}_g - p\dot{V} \right) . \quad (3)$$

The expression inside the brackets of equation (3) considers the power balance of the pressurized flow rate. The reciprocal volume before the bracket take account of the compressibility of the gas. The opening area of the valve is controlled by an underlying position controller. That guarantees proportionality between the opening area a and the set point voltage U :

$$a = c \cdot U, \quad (4)$$

where c is the specific ratio of the valve type. The supplied gas flow rate \dot{m}_g can be expressed [Bac89]:

$$\dot{m}_g = U \cdot c \cdot p_s \cdot \psi , \quad (5)$$

$$\text{with } \psi = \sqrt{\frac{2\eta}{RT_s(\eta-1)} \left[\left(\frac{p}{p_s} \right)^{\frac{2}{\eta}} - \left(\frac{p}{p_s} \right)^{\frac{\eta+2}{\eta}} \right]},$$

where η = specific heat ratio, p_s = supply pressure, T_s = supply temperature. This nonlinear valve characteristic was measured experimentally and shows a shifted zero line inside a dead zone due to the mechanical construction of the valve. In order to get a precise valve mapping, the characteristic curve was measured by inflating and deflating a closed pressure vessel using the valve. Dynamic effects of the underlying position controller for the valve-slide stroke are neglected. Assuming a constant supply pressure p_s , the mass flow is a numerical function ϕ of the pressure p inside the muscle and the set point voltage U :

$$\dot{m}_g = \phi(p, U) . \quad (6)$$

Next, it is necessary to describe the inner volume of the muscle. In this work the elastic and dynamic characteristics of the muscle's textile-fiber tubing are neglected. That means, the volume depends merely on the position and not on the pressure and its derivatives. By measuring the volume, one can approximate the volume as a polynomial function of third order depending on the position:

$$V(z) = \sum_{i=0}^3 b_i z^i . \quad (7)$$

The dynamic behavior of the trolley can be derived using Newtons second law:

$$m_s \ddot{z} = F_m - F_f - m_s g, \quad (8)$$

where F_m = longitudinal force of muscle, F_f = friction force of bearing, m_s = total trolley mass, \ddot{z} = acceleration

of slide, $g =$ gravitational constant. The frictional force F_f of the bearing is supposed to be a combination of coulomb friction $F_c = f_c \cdot \text{sgn}(\dot{z})$ and viscous friction $F_v = f_v \cdot \dot{z}$. In order to get an analytical function, the coulomb part of the friction is approximated by $F_c = f_c \cdot \tanh\left(\frac{\dot{z}}{\varepsilon}\right)$. Thus, the friction can be expressed as:

$$F_f(\dot{z}) = f_c \cdot \tanh\left(\frac{\dot{z}}{\varepsilon}\right) + f_v \cdot \dot{z} \quad . \quad (9)$$

An approximation of the muscle force for a McKibben pneumatic muscle has been derived by [Cho96]. The primary idea is to observe the energy conservation of mechanical and gas energy displacements:

$$dW_{mech} \stackrel{!}{=} dW_{gas} \quad . \quad (10)$$

As dynamical effects of the muscles textile-fiber tubing are neglected one can express: $dW_{mech} = F_m dz$ and $dW_{gas} = (p - p_0)dV$ [Cho96]. Thus, the muscle force can be written as:

$$F_m = (p - p_0) \cdot \frac{dV}{dz}, \quad (11)$$

where $p_0 =$ environment pressure. To calculate the force (11) it may be possible to use the relation in (7), however experimental results show large errors. Due to this, the function (11) is modified. With equation (11) the pneumatic muscle can be considered as an one way cylinder with flexible diameter. That means the expression $\frac{dV}{dz}$ in equation (11) could be interpreted as a variable piston area. Assuming that expression $\frac{dV}{dz}$ depends only on the length of the muscle [Lin99], [Cho96], the function of the force can be described as:

$$F_m(p, z) = (p - p_0) \cdot A(z), \quad (12)$$

where $A(z) =$ virtual piston area depending on the position. The piston area $A(z)$ is identified experimentally on the test stand as follows. Equation (12) yields for very slow movements with equation (8) with and (9):

$$A(z) = \frac{m_s g - f_c \cdot \tanh\left(\frac{\dot{z}}{\varepsilon}\right)}{p - p_0} \quad , \quad \text{for } p > p_0 \quad . \quad (13)$$

While the pressure is changed very slowly, the position and velocity of the slide are measured and the effective piston area can be calculated using function (13). This strategy is executed for different loads (e.g. between $m_s = 30kg$ and $m_s = 120kg$) and the results are used for a polynomial fit of fifth order. A higher polynomial order improves the accuracy of the curve fitting nonessential. As reported by [Neu01], the shape of this function decreases with the position in a monotonic manner. The muscle force can be expressed as:

$$F_m(p, z) = (p - p_0) \cdot \sum_{i=0}^5 c_i z^i \quad . \quad (14)$$

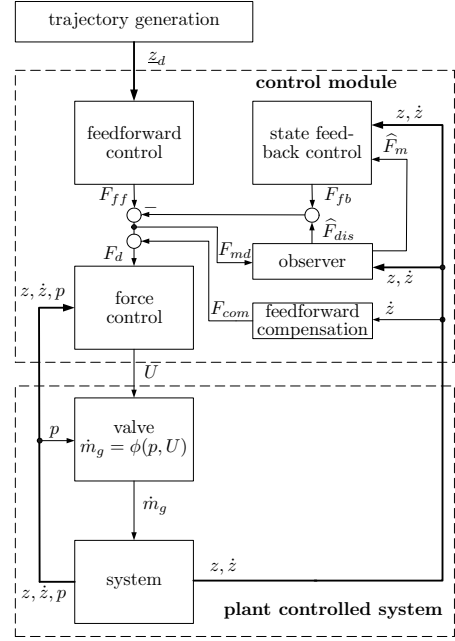


Fig. 3: Trajectory control structure with subsidiary force control.

Equations (7), (8), (9), (14) lead to the nonlinear system model of the experimental setup:

$$\begin{aligned} \dot{p} &= \frac{\chi}{3} \left(RT \dot{m}_g - \sum_{i=1}^3 i b_i z^{i-1} \cdot \dot{z} p \right) \\ &\quad \sum_{i=0} b_i z^i \\ \ddot{z} &= \frac{1}{m_s} \left((p - p_0) \cdot \sum_{i=0}^5 c_i z^i - f_c \cdot \tanh\left(\frac{\dot{z}}{\varepsilon}\right) \dots \right. \\ &\quad \left. \dots + f_v \cdot \dot{z} - m_s g \right) \quad . \end{aligned} \quad (15)$$

4 Controller Design

Core module of the control consists of a force control loop based on the inverse flow equation, inverse muscle-force function and the inverse valve characteristic. With an asymptotical tracking of the pressure, the force control assures a linear input/output behavior approximated by a first order delay element.

The trajectory tracking control comprises an observer based state feedback controller and a feedforward control. These modules guarantee a fast and vibration-free tracking of the position and ensure steady states in the desired position, velocity, acceleration and jerk. A compensation module cancels the weight of the trolley and the coulomb-part of the friction.

Figure 3 shows the layout of the control modules and system. The reference trajectory z_d is calculated by a trajectory planning module. In consideration of kinematical constraints it computes time indexed reference function for position, velocity, acceleration and jerk.

4.1 Force control

Defining the gas flow rate \dot{m}_g as output, equation (15) leads to the inverse flow:

$$\dot{m}_g = \frac{\sum_{i=0}^3 b_i z^i}{\chi RT} \left(\dot{p} + \frac{\chi \sum_{i=1}^3 i b_i z^{i-1}}{\sum_{i=0}^3 b_i z^i} \cdot \dot{z} p \right) . \quad (17)$$

With the measurement of the position z velocity \dot{z} and pressure p it can be easily proved that the flow equation satisfy the criteria for differential flatness [Fli92], [Fli93], [Rot96]. Hence, the pressure derivation is not part of the system it can be chosen freely:

$$\nu \stackrel{!}{=} \dot{p}, \quad (18)$$

where ν denotes the external reference input. This state feedback strategy compensates the nonlinearity of the flow equation to a first order integrator form [Isi95]. To stabilize the pressure, the external reference input is chosen so as to assure a vanishing tracking error $e = p_d - p$:

$$\nu = \dot{p}_d + K_p(p_d - p) \quad \text{with} \quad K_p > 0 , \quad (19)$$

where K_p specifies the control parameter and p_d denotes the desired pressure inside the muscle. Equations (17), (18) and (19) result to the nonlinear control function:

$$\dot{m}_g = \sum_{i=0}^3 b_i z^i \cdot \frac{\dot{p}_d + K_p(p_d - p)}{\chi RT} + \sum_{i=1}^3 i b_i z^{i-1} \cdot \frac{\dot{z} p}{RT}. \quad (20)$$

The desired pressure p_d can be expressed as the inverse muscle force function:

$$p_d = \frac{F_d}{\sum_{i=0}^5 c_i z^i} + p_0, \quad (21)$$

where F_d is the desired muscle force, which is calculated by the trajectory tracking controller. To derive the set point voltage of the valve according to the desired mass flow rate, the inverse valve characteristic (eq. (6)) is calculated numerically. By measuring the actual pressure p , the set point voltage of the valve can be expressed by: $U = \phi^{-1}(p, \dot{m}_g)$. Due to a dead zone of the valve response, the inversion causes a jump in the voltage. To get a homogeneous function, the dead zone is widened by a straight line.

The resulting structure of the force control can be seen in figure 4. The control input is the desired force which is converted to the corresponding pressure and derivative of the pressure. The nonlinear control is subject to an asymptotic pressure tracking, whereas the pressure inside the muscle, the position and velocity of the trolley are measured. The advantage of the presented force control is that it produce a linear input/output behavior:

$$F_m(s) = \frac{1}{1 + \frac{s}{K_p}} F_d(s) . \quad (22)$$

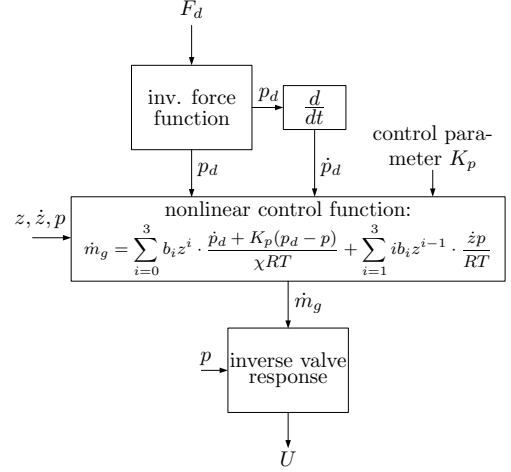


Fig. 4: Force control structure based on a nonlinear pressure control.

4.2 Trajectory tracking control

Feedforward compensation

The equations of motion (8)+(9) describe the time response of the position z :

$$F_m = m_s \ddot{z} + f_c \tanh\left(\frac{\dot{z}}{\varepsilon}\right) + f_v \dot{z} + m_s g \quad (23)$$

As the weight of the trolley and the coulomb part of the friction are time-constant (except at reversal or beginning movements) it is proposed to compensate it by a bias force (see figure 3): $F_{com} = m_s g + f_c$. Thus, the equation of motion is reduced to:

$$F_m = m_s \ddot{z} + f_v \dot{z} . \quad (24)$$

State feedback control design

The inverse Laplace transformation of transfer function (22) and the reduced equation of motion (24) lead to the linear state space representation:

$$\dot{\underline{x}} = \underline{A} \underline{x} + \underline{B} u, \quad y = \underline{C} \underline{x}, \quad (25)$$

where

$$\underline{A} = \begin{bmatrix} -K_p & 0 & 0 \\ 0 & 0 & 1 \\ m_s^{-1} & 0 & -f_v m_s^{-1} \end{bmatrix}, \underline{B} = \begin{bmatrix} K_p \\ 0 \\ 0 \end{bmatrix},$$

$$\underline{C} = [0 \ 1 \ 0], \underline{x} = [F_m \ z \ \dot{z}]^T, u = F_{md} .$$

In order to obtain an asymptotic tracking a state feedback control

$$F_{ff} = \underline{K} \underline{x} \quad (26)$$

is implemented. The feedback gains K_j are designed due to pole assignment P_j according to: $\prod_{j=1}^3 (s - P_j) \stackrel{!}{=} \det(s\underline{I} - \underline{A} + \underline{B} \underline{K})$, where \underline{I} is the identity matrix. Solving this equation system results to the feedback gains:

$$K_1 = -K_p m_s^{-1} f_v - K_p^{-1} (P_0 + P_2 + P_1) - 1$$

$$\begin{aligned}
K_2 &= -m_s K_p^{-1} P_0 P_1 P_2 \\
K_3 &= \left(m_s^{-1} f_v^2 - f_v (-P_0 - P_1 - P_2) + \dots \right. \\
&\quad \left. \dots m_s (P_0 P_2 + P_0 P_1 + P_1 P_2) \right) K_p^{-1}.
\end{aligned} \tag{27}$$

Observer design

The system state F_m needed for the state feedback control can't be measured. Therefore an observer has to estimate this state. In addition the observer is extended to a disturbance observer. Since the force control based on the inverse muscle force function, model errors of this function causes therefore a disturbance force F_{dis} . The transfer function of the force control (22) is expanded as follows:

$$F_m(s) = \frac{1}{1 + \frac{s}{K_p}} F_{md}(s) + \frac{1}{1 + \frac{s}{K_p}} F_{dis}(s) \quad . \tag{28}$$

The disturbance force is assumed to be piecewise constant:

$$\dot{F}_{dis} = 0 \quad . \tag{29}$$

The inverse Laplace transformation of transfer function (28), equation of motion (24) and equation (29) lead to the following linear state space representation:

$$\begin{bmatrix} \dot{\underline{x}}_{est} \\ \dot{\underline{x}}_m \end{bmatrix} = \begin{bmatrix} \underline{A}_{11} & \underline{A}_{12} \\ \underline{A}_{21} & \underline{A}_{22} \end{bmatrix} \begin{bmatrix} \underline{x}_{est} \\ \underline{x}_m \end{bmatrix} + \begin{bmatrix} \underline{B}_1 \\ \underline{B}_2 \end{bmatrix} u, \tag{30}$$

where the state vector $\underline{x}_{est} = [F_{dis} \ F_m]^T$ is to be estimated and the state vector $\underline{x}_m = [z \ \dot{z}]^T$ is measured, input function u equal to the desired muscle force F_{md} and the system matrices are:

$$\begin{aligned}
\underline{A}_{11} &= \begin{bmatrix} 0 & 0 \\ K_p & -K_p \end{bmatrix}, \underline{A}_{12} = \begin{bmatrix} 0 & 0 \\ 0 & 0 \end{bmatrix}, \underline{A}_{21} = \begin{bmatrix} 0 & 0 \\ 0 & m_s^{-1} \end{bmatrix}, \\
\underline{A}_{22} &= \begin{bmatrix} 0 & 1 \\ 0 & b m_s^{-1} \end{bmatrix}, \underline{B}_1 = [0 \ R_{Kraft}]^T, \underline{B}_2 = [0 \ 0]^T \quad .
\end{aligned}$$

Based on equation (30) it is designed a reduced-order observer according to:

$$\begin{aligned}
\dot{\underline{\rho}} &= (\underline{A}_{11} - \underline{H} \underline{A}_{21}) \underline{\rho} + (\underline{B}_1 - \underline{H} \underline{B}_2) u + \dots \tag{31} \\
&\dots ((\underline{A}_{11} - \underline{H} \underline{A}_{21}) \underline{H} + \underline{A}_{12} - \underline{H} \underline{A}_{22}) \underline{x}_m.
\end{aligned}$$

With the substitution:

$$\hat{\underline{x}}_{est} = \begin{bmatrix} \hat{F}_{dis} \\ \hat{F}_m \end{bmatrix} = \underline{\rho} + \underline{H} \underline{x}_m \tag{32}$$

it can be estimated the state vector $\hat{\underline{x}}_{est}$. The observer matrix \underline{H} are computed by pole assignment O_j according to: $\prod_{j=1}^2 (s - O_j) \stackrel{!}{=} \det(s\underline{I} - \underline{A}_{11} + \underline{H} \underline{A}_{21})$. Solving this equation system leads to the observer gains:

$$H_1 = H_3 = 0, H_2 = m_s K_p O_1 O_2, H_4 = m_s (O_1 + O_2 - K_p^{-1}). \tag{33}$$

The computed variable \hat{F}_m is then proceeded further to the state feedback control. The estimated disturbance force \hat{F}_{dis} is used to compensate model failures caused by the force control (see figure 3).

Feedforward control design

Realizing a feedforward control ensures vanishing steady state error for the position as well as for its first, second and third derivative. The feedforward control can be written as:

$$F_{ff} = \underline{V} \underline{z}_d = V_0 z_d + V_1 \dot{z}_d + V_2 \ddot{z}_d + V_3 \dddot{z}_d, \tag{34}$$

and is transformed into frequency domain:

$$F_{ff}(s) = (V_3 s^3 + V_2 s^2 + V_1 s + V_0) \cdot Z_d(s) \quad . \tag{35}$$

The transfer function of the closed loop system can be calculated by:

$$Z(s) = \underline{C}(s\underline{I} - \underline{A} + \underline{B} \underline{K})^{-1} \underline{B} \cdot F_{ff}(s) \quad . \tag{36}$$

Equation (36) combined with equation (35) lead to the complete system transfer function:

$$G(s) = \frac{V_3 s^3 + V_2 s^2 + V_1 s + V_0}{\frac{m_s}{K_p} s^3 + (K_1 m_s + \frac{f_v}{K_p} + m_s) s^2 + (f_v (K_1 + 1) + K_3) s + K_2} \tag{37}$$

The gains V_j are chosen in that way, that the coefficients of the numerator polynomial of $G(s)$ equal those of the denominator polynomial:

$$V_0 = K_2, V_1 = f_v (K_1 + 1) + K_3, V_2 = K_1 m_s + \frac{f_v}{K_p} + m_s, V_3 = \frac{m_s}{K_p}.$$

5 Experimental Results

To show the power of the presented control strategy, a plotted movement of the trolley with a total mass of $m_s = 90kg$ is presented in figure 5. Typical properties of the control are: dynamical tracking error of $e = 1 - 2mm$ and static tracking error of $e_{stat} = 10\mu m$. The lower plot of figure 5 shows the pressure history inside the muscle. Although the velocity of the trolley is constant, the pressure rises with the amount of the position in a nonlinear way. Figure 6 shows the difference between the deactivated and the activated control changing the payload mass stepwise from $m_s = 90kg$ to $m_s = 100kg$. In the case of the deactivated control the trolley is pretty low damped and position error up to $e = 20mm$ can be observed. In contrast to this, the activated control guarantees a good damping and low position errors. The disturbance observer estimates the error in force (lower plot) correctly of $\hat{F}_{dis} = -100N$.

6 Conclusion

A concept to control the position of payload is presented. As actuator it is used a pneumatic muscle which is produced by the manufacturer Festo. The used muscle possesses a high pulling force to 4000N and a long life period of at least 10 million switching cycles. For the control design a lumped substitute model for an experimental setup

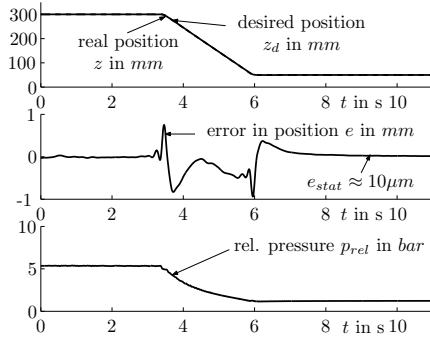


Fig. 5: Example of a movement (total slide mass: $m_s = 90\text{kg}$) from $z_d = 300$ to 50mm . Upper: desired and real position. Middle: tracking error. Lower: relative pressure inside the muscle.

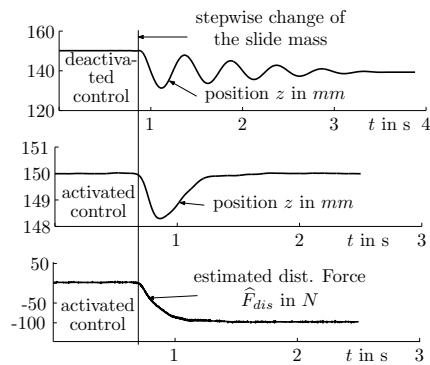


Fig. 6: Step response of the position error by changing the slide-mass stepwise from $m_s = 90\text{kg}$ to $m_s = 100\text{kg}$ (desired position $z_d = 150\text{mm}$). Upper: position z (deactivated control). Middle: position z (activated control). Lower: estimated disturbance force (activated control).

is derived. The physical states pressure inside the muscle, position and velocity of the slide describe the dynamical and static behavior of the setup. The limitation of the substitute model is, that the function of the muscle force based on experimental results and is therefore an approach. The model is characterized by nonlinearities. Thus, it is presented a nonlinear control concept consisting of an inner force control and an outer feedforward and an observer based feedback controller. The force control bases on a pressure tracking and compensates the whole nonlinearities of the system. Therefore the force control assures a linear input/output behavior approximated by a first order delay element. In order to get an asymptotic tracking of the position, it is implemented a linear observer based feedback control. To compensate model failures the observer is extended with a disturbance observer. The presented feedforward control ensures steady states concerning to the desired position, velocity, acceleration and jerk. Measurements prove the suitability of the control concept. A low static position error of $10\mu\text{m}$ demonstrates that pneumatic muscle can be used for high precision tasks in robotics.

References

- [Tak99] F. Takemura, S.R. Pandian, S. Kawamura, Y. Hayakawa, "Observer design for control of pneumatic cylinder actuators," in *"PTMC 99, Bath Workshop on Power Transmission and Motion Control"*, Bath, Sep 8.-10.9.1999, pp. 223-236, 1999.
- [Neu00] R. Neumann, J. Leyser, P. Post, "Simulationsgestützte Entwicklung eines servopneumatisch angetriebenen Parallelroboters," in *"SIM 2000, Dresdner Tagung Simulation im Maschinenbau, Softwaretools und Anwendungen in Lehre, Forschung und Praxis"*, Bd. 2, Dresden, 24.-25.2.2000 pp. 519-537, 2000.
- [Saw02] O. Sawodny, A. Hildebrandt, "Aspects of the control of differential pneumatic cylinders," in *10th Japanese-German Seminar on Nonlinear Problems in Dynamical Systems*, Kanazawa, pp 247-256, 2002.
- [Hil02] A. Hildebrandt, O. Sawodny, R. Neumann, A. Hartmann, "A flatness based design for tracking control of pneumatic muscle actuator", *Seventh International Conference on Control, Automation, Robotics & Vision*, Singapore, pp 1156-1161, 2002
- [Tao96] G. Tao, P.V. Kokotovic, "Adaptive control of systems with actuator and sensor nonlinearities", in *John Wiley & Sons, INC., New York*, 1996.
- [Tan99] G. Tanaka, Y. Yamada, T. Satoh, A. Uchibori, S. Uchikado, "Model Reference Adaptive Control with Multi-Rate Type Neural Network for Electro-Pneumatic Servo System", in *Proc. IEEE International Conference on Control Applications*, Hawaii, pp. 1716-1721, 1999.
- [Rep99] D. W. Repperger, K. R. Johnson, C. A. Philips, "Nonlinear feedback controller design of a pneumatic muscle actuator system," in *Proc. 1999 American Control Conference*, San Diego, pp. 1525-1529, 1999.
- [Lin99] R. Q. van der Linde, "Design, analysis, and control of a low power joint for walking robots, by phasic activation of McKibben muscles," in *Proc. IEEE Transactions on Robotics and Automation*, Vol. 15, No. 4, pp. 599-604, 1999.
- [Cho96] C. P. Chou, B. Hannaford, "Measurement and modeling of McKibben pneumatic artificial muscle," in *Proc. IEEE Transactions on Robotics and Automation*, Vol. 12, No. 1, pp. 90-102, 1996.
- [Neu01] R. Neumann, M. Göttert, "Roboter mit servopneumatischen Antrieben," in *Proc. 4. Deutsch-Polnisches Seminar "Innovation und Fortschritt in der Fluidtechnik"*, Sopot, pp. 205-223, 2001.
- [Bac89] W. Backe, O. Ohligschlager, "A model of heat transfer in pneumatic chambers," in *Journal of Fluid Control*, Vol. 20, No. 1, pp. 67-78, 1989.
- [Fli92] M. Fliess, J. Levine, Ph. Martin, and P. Rouchon, "Sur le systèmes non linéaires différentiellement plats," in *C.R. Acad. Sci. Paris*, t. 315, Série I, pp. 619-624, 1992.
- [Fli93] M. Fliess, J. Levine, Ph. Martin, and P. Rouchon, "Linéarisation par bouclage dynamique et transformations de Lie-Bäcklund," in *C.R. Acad. Sci. Paris*, t. 317, Série I, pp. 981-986, 1993.
- [Rot96] R. Rothfuß, J. Rudolph, and M. Zeitz, "Controlling a chemical reactor model using its flatness," in *Proc. 13th IFAC World Congress*, San Fransisco, Vol. F, pp. 383-388, 1996.
- [Isi95] A. Isidori, "Nonlinear control systems," Springer Verlag, 3rd edition, 1995.